Self-diffusion micromechanism in Nafion studied by ^{2}H NMR relaxation dispersion

Elena A. Galitskaya, (iD) Alexei F. Privalov, (iD) Michael Vogel, (iD) Ivan A. Ryzhkin, and (iD) Vitaly V. Sinitsyn

View Online   Export Citation   CrossMark

ARTICLES YOU MAY BE INTERESTED IN

Self-diffusion micromechanism in Nafion studied by ^{2}H NMR relaxation dispersion

View Online   Export Citation   CrossMark

Elena A. Galitskaya,[1,2] Alexei F. Privalov,[1] ![ID] Michael Vogel,[1] ![ID] Ivan A. Ryzhkin,[2] ![ID] and Vitaly V. Sinitsyn[2,3,a] ![ID]

AFFILIATIONS

[1] Institute of Condensed Matter Physics, Technische Universität Darmstadt, Hochschulstr. 6, 64289 Darmstadt, Germany
[2] Institute of Solid State Physics RAS, 2 Academician Ossipyan Str., 142432 Chernogolovka, Russian Federation
[3] Inenergy Group LLC, Electrodnaya Str., 12-1, 111524 Moscow, Russian Federation

[a] Author to whom correspondence should be addressed: sinitsyn@issp.ac.ru

ABSTRACT

Field Cycling (FC) ^{2}H nuclear magnetic resonance (NMR) relaxometry was applied to study dynamics in Nafion NR 212 in the temperature range from 300 K to 190 K and water content of λ = 8.2. The sensitive time window of FC was extended up to eight decades using the temperature–frequency superposition principle and master curve. The rotational correlation times obtained from ^{2}H FC NMR coincide with translational correlation times gained from static field ^{2}H NMR diffusometry in the temperature range applied. This fact means that a long-range mass transport in Nafion is coupled to molecular rotations. It is assumed that confined water in Nafion has more ordered oxygen sublattices as compared with bulk water, on a short range is similar to ice. We discuss the possible role of D and L defects, typical for the ordered ice structure and using this concept to describe the processes of self-diffusion of confined water in Nafion, as well as the similarity of temperature and humidity dependence of self-diffusion and proton conductivity.

Published under license by AIP Publishing. https://doi.org/10.1063/5.0036605

I. INTRODUCTION

The dynamic properties of confined water are of great importance for understanding the transport processes in various polymers, minerals, and biological systems.[1–9] Proton-exchange membranes are undoubtedly of interest in this regard because the water in them is confined in nanochannels with a diameter of ~1 nm to 5 nm. The study of confined water dynamics in Nafion vs temperature and water content λ (λ = N_{H2O}/N_{SO3}) provides a wide field (see a recent review[10] and references therein). The proton conductivity in Nafion at room temperature and high humidity (~100%) can reach 0.1 S/cm, thus making these polymers attractive for application in various electrochemical devices.[10–13] However, these polymers have found the greatest commercial success as the proton-exchange membranes for hydrogen fuel cells (PEMFCs).[10,14–16] In these devices, the proton conductivity occurs in wide temperature and humidity ranges, both important for PEMFC performance.

Another parameter important for the stability of PEMFC operation and for the performance in gas humidification and water drainage is the self-diffusion coefficient of water.[10,14–16] To determine the self-diffusion coefficients in perfluorinated sulfopolymers, several methods have been applied.[10,14,17–21] One of the most convenient and reliable methods is nuclear magnetic resonance (NMR) diffusometry in applied magnetic field gradients, which is a non-invasive and isotope (^{1}H or ^{2}H) selective method.[10,17–21]

The results of ^{1}H NMR diffusometry were compared with those of proton conductivity for Nafion at room temperature.[17] It was shown that the NMR self-diffusion coefficients (D_{NMR}) and those calculated from the *dc* conductivity using the Nernst–Einstein relation (D_σ) are in agreement, explicitly D_{NMR}/D_σ ~0.5–2, and change in a similar way when the water content is varied.[10,17–20] Moreover, it was found[21] that the temperature dependencies of proton conductivity and self-diffusion coefficients are nearly identical for Nafion at a fixed value of λ. It should be noted that D_{NMR} is about four times smaller than D_σ in bulk water at room temperature.[22] The reasons for the different D_{NMR}/D_σ ratios of water in Nafion and in the bulk are not explicitly discussed in the literature.

Another important difference of water behaviors in Nafion and in the bulk relates to the isotope effect (IE) associated with the

change in the diffusion coefficients upon substitution of H_2O by D_2O (hereinafter, D^H and D^D). For Nafion at $\lambda = 8.2$, the IE is 1.4 in a wide temperature range.[23] This value is close to the square root of 2, which is the "classical" value for H^+ ion migration and is usually explained by the change in the attempt frequency to overcome a potential barrier under the assumption of a small influence of the ground state energy on the activation energy.[24–27] If the "classical" case is applied to the water molecules, the IE on the self-diffusion should amount to ~1.05 (the square root of the mass ratio of D_2O and H_2O). The measured IE value for bulk water at room temperature is close to 1.23 with a tendency to increase with decreasing temperature.[24]

Remarkably, the IE should have a value close to $\sqrt{2}$ also for the rotation of $H(D)_2O$ molecules as a whole. Hence, water reorientation may be important for the long-range mass transport in Nafion.[28,29] Specifically, the rotational correlation times of D_2O and H_2O (τ_{rot}^D and τ_{rot}^H) should be related to the respective molecular moments of inertia (I^D and I^H) according to the following equation:[24]

$$\tau_{rot}^D = \tau_{rot}^H \sqrt{\frac{I^D}{I^H}}. \tag{1}$$

Because the oxygen atom is close to the center of mass and the O–H and O–D distances are nearly identical, $\sqrt{I^D/I^H}$ is close to the square root of 2 (it is in the range of 1.36–1.41 for the three main axes[24]). Thus, we can hypothesize based on the matching of the isotope effect of translational diffusion with the rotational moment of the inertia isotopic ratio that molecular rotation is significant for the diffusion processes in Nafion, and it is interesting to analyze the relation in more detail.

A well-suited method for this purpose is NMR relaxometry, which involves the measurement of spin-lattice relaxation (SLR) time T_1 for various Larmor frequencies ν. Nowadays, Field Cycling (FC) NMR relaxometry[30,31] provides access to $T_1(\nu)$ dispersions over broad frequency ranges. In this way, molecular dynamics (MD) can be studied on a microscopic scale and over wide dynamic and temperature ranges. In particular, FC NMR was successfully applied to various complex systems, such as liquid crystals, biological systems, and polymers.[32]

[1]H FC relaxometry was also applied to investigate water dynamics in Nafion.[33–36] An analysis of $T_1(\nu)$ dispersion curves suggested that there are two types of bound water.[33] The first type is only found in the driest samples and possesses considerably reduced mobility, and the second type is common to all samples and corresponds to the expected bound water. Moreover, ^{1}H FC relaxometry was employed to measure the frequency dependence of T_1 for Nafion 112 at three hydration levels: $\lambda \approx 3.7$, $\lambda \approx 5.6$, and $\lambda \approx 10.6$.[35] The authors assumed that the anisotropy of the diffusion observed at a low hydration level is related to a local structural organization involving biaxial aggregates forming lamellar domains at the nanometer scale. ^{2}H NMR SLR times were measured at several Larmor frequencies ν to characterize D_2O dynamics in Nafion 117.[34] The authors concluded that at low hydration, the molecular motions of D_2O are affected by the acidity and mobility of the sulfonic acid groups to which the water molecules are coordinated. Under such circumstances, the acidity and mobility of sulfonic acid groups have a main influence on water dynamics. At higher hydration levels, the molecular motion of D_2O is affected by the phase separation of the

hydrophilic/hydrophobic domains and the size of the hydrophilic domains. The combination of ^{1}H NMR spectroscopy, relaxometry, and diffusometry allows authors[36] to distinguish two motional modes for water in Nafion 117 at a low hydration level, where non-freezing behavior of water molecules takes place. A comparison of long- and short-range motion studies revealed the hydration shell formation for the sulfonic acid groups that can be divided into three characteristic regions: the formation of the first hydration shell at $\lambda \approx 3$, that of the second hydration shell at $\lambda \approx 8$, and the presence of bulk water above $\lambda \geq 10$.[36]

Despite the capabilities of ^{1}H relaxometry, it has some disadvantages. The protons are subject to both intra- and intermolecular dipolar interactions among neighboring spins so that ^{1}H SLR is affected by the fluctuations of both types of interactions and, hence, by rotational and translational motions of the molecules. Therefore, it is difficult to single out the information about rotational dynamics. Another drawback of ^{1}H relaxometry is the influence of paramagnetic impurities, which yield significant contributions to ^{1}H SLR in Nafion, especially at elevated temperatures, masking dynamical contributions. In these respects, ^{2}H relaxometry studies of systems containing D_2O are of advantage because, for deuterons, the quadrupole interaction dominates, which probes changes in the orientation of the D–O bond.[30–32,34,37] Therefore, ^{2}H SLR studies allow for a determination of D_2O rotational correlation times τ_{rot}. However, the capabilities of, in particular, ^{2}H FC relaxometry have not yet been exploited for a detailed analysis of D_2O rotational dynamics in Nafion.

For this reason, we carried out ^{2}H FC NMR measurements on Nafion samples loaded with heavy water. The main goal of this work is an experimental investigation of the influence of local rotational dynamics of water on the long-range mass transport in Nafion. For this purpose, we compare the present ^{2}H FC NMR relaxometry results with the findings of a previous ^{2}H static field gradient (SFG) NMR study,[23] which analyzed diffusion on a length scale of ~1 μm. Specifically, the ^{2}H FC relaxometry studies are carried out on a Nafion NR 212 membrane with a D_2O hydration level of $\lambda \approx 8.2$, the same that we have used in the ^{2}H FG diffusometry measurements.[23]

II. EXPERIMENTAL DETAILS

A. Sample preparation

The Nafion NR 212 membrane was purchased from Chemours (USA). The cleaning was done in the same way as proposed in Ref. 17. The cleaned membrane was cut into 1×5-cm stripes to fit in the standard 5 mm NMR tube. Finally, the sample was dried at 298 K below 5×10^{-6} mbar for 48 h. To obtain the desired water content, the membrane stripes were placed in a desiccator containing a saturated solution of $KBrO_3$ salt solved in D_2O, thus producing around 98% of RH. The desiccator was darkened and kept at the temperature of 296 K. It was found that the weight of the samples became stable after 14 days of wetting. Afterward, the sample was quickly inserted into the NMR tube, which was then closed by a teflon cap and sealed with a small amount of epoxy resin to avoid water loss. The weight of sample was the same during all measurements, ensuring that the water concentration was constant.

B. Field cycling relaxometry

NMR SLR times T_1 are sensitive to molecular motions. Generally, the SLR rates T_1^{-1} are determined by spectral density function J_2, which is the Fourier transform of a time correlation function characterizing stochastic temporal fluctuations of the interatomic interactions. If T_1 measurements are restricted to a single Larmor frequency, the only experimental parameter that can be varied is the sample temperature. Then, correlation time τ can be obtained from the position of the T_1 minimum in a temperature scan, while information about the shape of the spectral density is not available. FC relaxometry is a much more informative tool because the Larmor frequency can be varied in a broad range and the frequency dependent SLR rates $T_1^{-1}(\nu)$ can be recorded, which are essentially proportional to $J_2(\nu)$. Thus, the spectral densities of dynamic processes at every accessible temperature can be traced. In the FC experiment, the applied magnetic field is rapidly switched between polarization, relaxation, and detection fields, enabling SLR measurements for ^{1}H frequencies from typically ~30 MHz down to several Hz and, thus, in an ~7 orders of magnitude broad frequency range.[38]

Our ^{2}H T_1 measurements were performed using a home-built FC relaxometer, which was described in detail in previous works.[30,31] Briefly, the magnetic field is created by using a resistive low inductive solenoidal system powered with a high voltage switching power amplifier, allowing for short switching times.[30] A polarization field corresponding to the ^{2}H NMR frequency of 5 MHz and a detection field of 11.5 MHz were used. Relaxation was measured for the magnetic field range from 3 kHz to 5 MHz. The 90° pulse length was 3 μs. The buildup of magnetization was determined from the amplitude of the free induction decay after the 90° pulse. These FC data were supplemented by additional saturation-recovery T_1 measurements in standard superconducting magnets at fixed frequencies of 9.2 MHz, 14 MHz, and 46 MHz. The investigations were carried out in the temperature range from 190 K to 300 K. The temperature was set with an accuracy of 1 K and stabilized with an accuracy of ±0.5 K. The magnetization decays were monoexponential over the whole temperature range. From 64 to 128 accumulations were used to reach an accuracy of T_1 better than 5%.

To further extend the time window of FC NMR, we exploit that frequency–temperature superposition applies.[38] Explicitly, when the shape of the spectral density $J_2(\nu)$ does not change in the studied temperature range, master curves can be constructed by shifting the experimental data measured at various temperatures along the frequency axes. Moreover, we use the fluctuation–dissipation theorem to switch from a spectral-density to a dynamic-susceptibility representation of the measured $T_1(\nu)$ dispersions.[39] In this theoretical framework, both quantities are related according to $\chi''(\omega) = \omega J(\omega)$. Thus, based on the Bloembergen–Purcell–Pound relation, an NMR susceptibility can be defined according to the following equation:

$$\omega/T_1(\omega) = C\left[\chi''(\omega) + 2\chi''(2\omega)\right] = C\chi''_{NMR}(\omega), \qquad (2)$$

where C is the NMR coupling constant. This NMR susceptibility can be interpreted in analogy with its mechanical and electrical counterparts. Specifically, the peak position provides straightforward access to the characteristic time constant of the dynamical process, and the peak width informs about a possible nonexponentiality of the relaxation, e.g., because of dynamical heterogeneity.

III. RESULTS

The correlation times of water molecules in Nafion at ambient temperature are much shorter than the time window of ^{2}H FC NMR, which ranges typically from 10^{-3} to 10^{-7} c. Therefore, we extend this time window to shorter correlation times by additional T_1 measurements at higher frequencies using superconducting magnets. ^{2}H T_1 dispersions at various temperatures are presented in susceptibility representation, $\nu T_1^{-1}(\nu)$, in Fig. 1. At low temperatures and low frequencies, the T_1 times are shorter than 1 ms, which leads to relaxation during the field switches so that the difference between the signal amplitudes at the beginning and at the end of the relaxation period, the so called "contrast," does no longer exceed the noise level, making T_1 measurements impossible.[32] For this reason, we show only the reliable T_1 values in Fig. 1. It can be seen that, down to 220 K, the susceptibility values continuously increase to higher frequencies, indicating that the motion is fast on the time scale of the experiment. At the lowest temperature of 190 K, a maximum of $\nu T_1^{-1}(\nu)$ is observed at ν_{max} = 10 MHz, indicating that the rotational correlation time is of the order of the inverse of this frequency.

Following the common procedure in electrical and mechanical relaxation studies, we assume frequency–temperature superposition to further extend the time window by construction of a master curve. Specifically, we shift the susceptibility curves for different temperatures along the frequency axis to the curve, for which the susceptibility maximum is observed (in our case, 190 K), until the optimum overlap is reached, as presented in Fig. 2. As one can see, the susceptibilities for the individual temperatures nicely collapse onto a single master curve, thus supporting the assumption of temperature–frequency superposition for the system under investigation. In this way, the dynamic range of our FC approach can be extended to almost 8 decades.

The susceptibility maximum occurs when the rotational correlation amounts to $\tau_{rot} \approx 0.6/2\pi\nu_{max}$. The correlation times for other temperatures can be calculated from the shift factors used to construct the master curves. The errors of relative τ_{rot} gained using frequency–temperature superposition treatment are on the level of
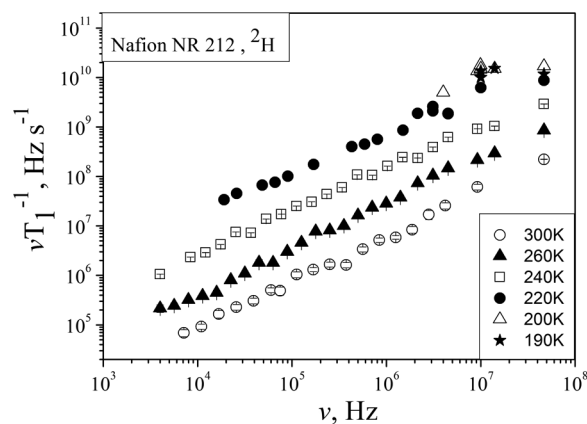

FIG. 1. ^{2}H NMR T_1 dispersions for Nafion NR 212 saturated with D_2O at $\lambda \approx 8.2$ in susceptibility representation, νT_1^{-1}.
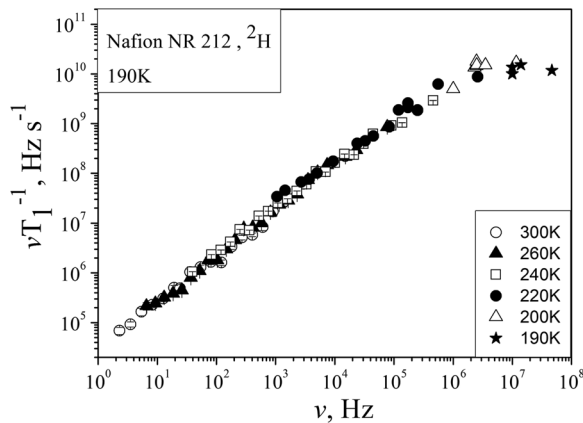
FIG. 2. Master curve of the ^{2}H FC NMR susceptibilities for Nafion NR 212 saturated with D$_2$O at $\lambda \approx 8.2$.
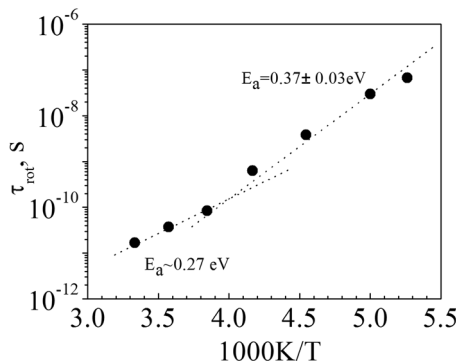

FIG. 3. Temperature-dependent rotational correlation times τ_{rot} for D$_2$O in Nafion NR 212 at $\lambda \approx 8.2$.

5%, while the absolute error is higher and can be estimated as 10%. The correlation times gained in this way are presented in Fig. 3.

Two temperature regimes for τ_{rot} with activation energies of $E_a(\tau_{rot}) \sim 0.27$ eV above ~250 K and $E_a(\tau_{rot}) \approx 0.37 \pm 0.03$ eV below 250 K can be identified in Fig. 3. These temperature ranges were chosen by analogy with the temperature dependencies of diffusion coefficient D$_{NMR}$ of various perfluorosulfonated membranes investigated in Ref. 21. The activation energy of $E_a(\tau_{rot}) \approx 0.37 \pm 0.03$ eV for the low-temperature interval is in good agreement with the activation energies 0.34 eV–0.37 eV of the self-diffusion coefficient below the crossover temperature.[21] At high temperatures (above crossover point), the activation energy $E_a(\tau_{rot}) \sim 0.27$ eV was calculated using only three experimental points and can actually be considered as estimation, requiring further refinement.

IV. DISCUSSION

To understand the relevance of the rotational motion for the macroscopic diffusion, we compare rotation correlation times τ_{rot}

with correlation times τ_{dif} calculated from the ^{2}H diffusion coefficients measured in previous work.[23] For this purpose, one has to take into account the tortuous trajectory of water molecules in Nafion. The tortuosity factor characterizes a decrease in the diffusion coefficient on pathways in the polymer matrix in comparison with a free random walk of the water molecule. In the first approximation, this parameter can be considered as a geometric factor.[40,41] Experimentally, this parameter was found to be around 2 for Nafion at high water content, $\lambda \geq 6$.[18] The value of $\beta = 2$ was taken for further calculations in the assumption of 3D isotropic H$_2$O diffusion. Thus, τ_{dif} can be defined as

$$\tau_{dif} = \frac{l^2}{6\beta D^D}, \qquad (3)$$

where l is the D$_2$O jump length, which is 0.28 nm,[40] and D^D is the self-diffusion coefficient of D$_2$O molecules.[23] The jump length of water molecule is usually identified as a nearest O–O distance. According to experimental data,[42] this parameter is in the range of 0.275 nm–0.294 nm,[42] but usually, the 0.28 nm jump length is accepted, and we used it in our calculations. The influence of O–O distance spread on calculated τ_{dif} is within the range of 5%. Thus, using currently available data on D$_2$O diffusion, tortuosity, and jump length, an accuracy of gained τ_{dif} times we estimate is 10%.

Because the diffusion measurements of D^D were restricted to 240 K, the comparison of the correlation times of reorientation τ_{rot} and diffusion τ_{dif} is limited to this temperature range in Fig. 4.

It can be clearly seen from Fig. 4 that the correlation times of the rotational and diffusive motions agree with the studied temperature range, and hence, every rotational jump of D$_2$O in Nafion NR 212 is coupled to a translational jump relevant for the long-range mass transport. Such a rotational–translation coupling is proposed by using a model.[43] This close relation between the rotational and diffusive motions of D$_2$O in Nafion NR 212 can be compared with the situation in bulk water.

The rotational diffusion mechanism in bulk water has been intensively studied both experimentally[24,44,45] and theoretically.[46,47] In water, the IE for the self-diffusion coefficient is $D^H/D^D = 1.23$. The deviation from the "classical" value of square root of 2 (~1.41)
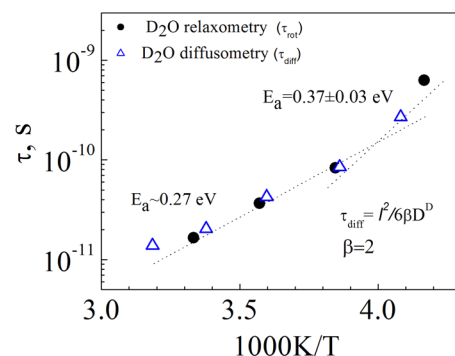

FIG. 4. Comparison of rotational correlation times from ^{2}H FC relaxometry and diffusion correlation times from ^{2}H SFG diffusometry for Nafion NR 212 loaded with D$_2$O at $\lambda = 8.2$. The latter are calculated from the self-diffusion coefficients using Eq. (3). The data are presented in the mutually intersection temperature regions of measurements.

is explained by the translational–rotational coupling mechanism, which actually corresponds to the proximity of the correlation times of translation and rotation of the molecule.[24] The mechanism for the rotational motion involves the molecules' large angular jumps (~60°) with the formation of an intermediate state having a bifurcated hydrogen bond (defect with five H-bonds), followed by the simultaneous breakage of the previous bond and the formation of a new hydrogen bond.[44,45] However, this mechanism provides only the displacements of the protons not that of the entire water molecule. Thus, the mechanism for self-diffusion in water is still not fully specified theoretically.

As aforementioned, water in proton-exchange membranes is in a confined state with a structure, which has noticeably higher oxygen order than that of bulk water and, thus, approaches the structure of ice.[48–53] Recently, it was also demonstrated by means of MD simulations that water becomes ordered and solid-like at some size of the hydrophilic domains in the perfluorosulfonic acid membrane.[54] This allows us to use Jaccard's theory, originally developed for ice, to describe the confined state of water in Nafion.[50–53] According to this theory, the dynamic electrical properties of ice (complex dielectric permittivity, Debye relaxation, and frequency dependence of the proton conductivity) can be described in terms of proton point defects, which violate the ice rules and include two mechanisms:

- Ionic H_3O^+ and OH^- defects with the excess or lack of a proton, respectively.
- Bond D and L defects when there are two or zero protons along the hydrogen bond, respectively.

Ionic defects are responsible for the charge transfer and low-frequency proton conductivity, whereas bond defects are responsible for the self-diffusion of water molecules, high-frequency conductivity, and dielectric relaxation.[50–53,55–57] Moreover, the D-defects can be considered as interstitial defects where the water molecules are located in a cavity formed by hexagonal arrangements of neighbors.[58,59] Therefore, the self-diffusion of confined water can be described using phenomenological approaches developed for the crystal structures, where point defects (interstitial ions and vacancies) are responsible for the transport characteristics.[59,60]

It can be assumed that the process of self-diffusion in bulk and confined water is caused by the migration of D and L defects, where D defects can be associated with interstitial molecules and L defects with vacancies. The D defect migration occurs via molecular jumps over local energy barriers, separating minima in the cavities of the hexagonal rings, whereas L defect migration occurs via molecular jumps owing to broken H-bonds.

Recently, we proposed an analytical model describing the behavior of water in mesoporous media.[52,53] The main conclusion of this model is that the 5 orders of magnitude higher proton conductivity in Nafion than in bulk water is due to a significant increase in the concentration of proton charge carriers, while the proton mobility itself is not much affected. According to Jaccard's theory, the protonic transport, which is responsible for the *dc* conductivity, involves alternating motion of ionic defects (H_3O^+ and OH^-) and bond defects (D and L). In bulk ice and bulk water, the concentration of ionic defects is 5–6 orders of magnitude lower than the concentration of bond defects so that the involvement of the ionic defects is the limiting factor for the dc conductivity.[50–53]

The situation is different in Nafion NR 212 where the water is located in nanochannels containing SO_3^- groups, and hence, the concentration of ionic defects is similar or even higher than the concentration of bond defects.[52] Therefore, the availability of bond (D and L) defects may become the limiting factor for proton transfer.[60,61] Some differences for coefficients D_σ and D_{NMR} at different λ can be due to different contributions of ion (H_3O^+, OH^-) and bond (L, D) defects to proton conductivity, whereas only bond defects take part in diffusion micromechanism.

V. CONCLUSION

^{2}H FC NMR relaxometry was applied to study the local D_2O molecular dynamics in Nafion NR 212 in a wide frequency range. Unlike the ^{1}H analog, the present ^{2}H approach is exclusively sensitive to molecular rotations because it probes the fluctuations of the quadrupolar interaction, which is of intramolecular nature and depends on the molecular orientation with respect to the applied magnetic field. We have found that frequency–temperature superposition applies to D_2O reorientation in Nafion NR 212, enabling a construction of master curves. In this way, the rotational correlation times have been determined in a broad temperature range from 300 K to 190 K, and the associated activation energies have been obtained. The ^{2}H FC relaxometry data have been compared with ^{2}H SFG diffusometry results for the same sample.[23] The comparison showed that the correlation times of rotational and translational motions coincide (within experimental errors) in the temperature range from 290 K to 230 K, and hence, molecular reorientations play an important role in the self-diffusion of D_2O in Nafion NR 212. Similar conclusions were drawn recently based on isotope effects for self-diffusion.[23] We propose that the microscopic mechanism for the self-diffusion of the confined water is described by a modified Jaccard's theory, which involves both ionic defects (H_3O^+ and OH^-) and bond defects (D and L). It allows for a phenomenological explanation of the similar dependence of the ionic conductivity and self-diffusion in Nafion NR 212 on temperature and water content.

ACKNOWLEDGMENTS

DATA AVAILABILITY

The data that support the findings of this study are available within the article.

REFERENCES

[1] K. L. Ngai, S. Capaccioli, and A. Paciaroni, Chem. Phys. **424**, 37 (2013).
[2] J. Swenson and S. Cerveny, J. Phys.: Condens. Matter **27**, 033102 (2015).
[3] H. E. Stanley, S. V. Buldyrev, G. Franzese, P. Kumar, F. Mallamace, M. G. Mazza, K. Stokely, and L. Xu, J. Phys.: Condens. Matter **22**, 284101 (2010).
[4] M. Weigler, M. Brodrecht, G. Buntkowsky, and M. Vogel, J. Phys. Chem. B **123**, 2123 (2019).
[5] Y. Yao, V. Fella, W. Huang, K. A. I. Zhang, K. Landfester, H.-J. Butt, M. Vogel, and G. Floudas, Langmuir **35**, 5890 (2019).
[6] C. Lederle, M. Sattig, and M. Vogel, J. Phys. Chem. C **122**, 15427 (2018).

[7] M. Weigler, M. Brodrecht, H. Breitzke, F. Dietrich, M. Sattig, G. Buntkowsky, and M. Vogel, Z. Phys. Chem. **232**, 1041 (2018).

[8] X. Meng, H.-N. Wang, S.-Y. Song, and H.-J. Zhang, Chem. Soc. Rev. **46**, 464 (2017).

[9] H. Yao, H. Ke, X. Zhang, S.-J. Pan, M.-S. Li, L.-P. Yang, G. Schreckenbach, and W. Jiang, J. Am. Chem. Soc. **140**, 13466 (2018).

[10] A. Kusoglu and A. Z. Weber, Chem. Rev. **117**, 987 (2017).

[11] J.-S. Jiang, D. B. Greenberg, and J. R. Fried, J. Membr. Sci. **132**, 255 (1997).

[12] H. L. Yeager and A. A. Gronowski, *Ionomers* (Springer Netherlands, 1997), pp. 333–364.

[13] Z. Fan and D. J. Harrison, Anal. Chem. **64**, 1304 (1992).

[14] K.-D. Kreuer, T. Dippel, W. Meyer, and J. Maier, MRS Proc. **293**, 273 (1992).

[15] K. D. Kreuer, J. Membr. Sci. **185**, 29 (2001).

[16] K. A. Page and B. W. Rowe, in *ACS Symposium Series* (American Chemical Society, 2012), pp. 147–164.

[17] T. A. Zawodzinski, M. Neeman, L. O. Sillerud, and S. Gottesfeld, J. Phys. Chem. **95**, 6040 (1991).

[18] Q. Zhao, P. Majsztrik, and J. Benziger, J. Phys. Chem. B **115**, 2717 (2011).

[19] F. Xu, S. Leclerc, O. Lottin, and D. Canet, J. Membr. Sci. **371**, 148 (2011).

[20] S. Ochi, O. Kamishima, J. Mizusaki, and J. Kawamura, Solid State Ionics **180**, 580 (2009).

[21] E. Galitskaya, A. F. Privalov, M. Weigler, M. Vogel, A. Kashin, M. Ryzhkin, and V. Sinitsyn, J. Membr. Sci. **596**, 117691 (2020).

[22] K.-D. Kreuer, Chem. Mater. **8**, 610 (1996).

[23] A. F. Privalov, E. Galitskaya, V. Sinitsyn, and M. Vogel, Appl. Magn. Reson. **51**, 145 (2020).

[24] E. H. Hardy, A. Zygar, M. D. Zeidler, M. Holz, and F. D. Sacher, J. Chem. Phys. **114**, 3174 (2001).

[25] A. N. Murin, I. V. Murin, and V. I. Portnyagin, Russ. Chem. Rev. **49**, 968 (1980).

[26] V. V. Sinitsyn, E. G. Ponyatovskii, A. I. Baranov, A. V. Tregubchenko, and L. A. Shuvalov, Sov. Phys. JETP **73**, 386 (1991).

[27] S. M. Haile, D. L. West, and J. Campbell, J. Mater. Res. **13**, 1576 (1998).

[28] N. Agmon, J. Chim. Phys. **93**, 1714 (1996).

[29] N. Agmon, Chem. Phys. Lett. **244**, 456 (1995).

[30] O. Lips, A. F. Privalov, S. V. Dvinskikh, and F. Fujara, J. Magn. Reson. **149**, 22 (2001).

[31] B. Kresse and A. F. Privalov, *New Developments in NMR* (Royal Society of Chemistry, 2018), pp. 88–117.

[32] R. Kimmich, *Field-Cycling NMR Relaxometry Instrumentation, Model Theories and Applications* (Royal Society of Chemistry, 2019).

[33] F. Xu, S. Leclerc, and D. Canet, J. Phys. Chem. B **117**, 6534 (2013).

[34] D. K. Lee, T. Saito, A. J. Benesi, M. A. Hickner, and H. R. Allcock, J. Phys. Chem. B **115**, 776 (2011).

[35] J.-C. Perrin, S. Lyonnard, A. Guillermo, and P. Levitz, J. Phys. Chem. B **110**, 5439 (2006).

[36] R. Hammer, M. Schönhoff, and M. R. Hansen, J. Phys. Chem. B **123**, 8313 (2019).

[37] T. M. Kirschgen, M. D. Zeidler, B. Geil, and F. Fujara, Phys. Chem. Chem. Phys. **5**, 5243 (2003).

[38] B. Kresse, M. Becher, A. F. Privalov, M. Hofmann, E. A. Rössler, M. Vogel, and F. Fujara, J. Magn. Reson. **277**, 79 (2017).

[39] M. Flämig, M. Hofmann, and E. A. Rössler, Mol. Phys. **117**, 877 (2019).

[40] S. Koter, J. Membr. Sci. **206**(1-2), 201 (2002).

[41] K. Chang, A. Korovich, T. Xue, W. A. Morris, L. A. Madsen, and G. M. Geise, Macromolecule **51**, 9222 (2018).

[42] P. L. Silvestrelli and M. Parrinello, J. Chem. Phys. **111**, 3572 (1999).

[43] D. Chandler, J. Chem. Phys. **62**, 1358 (1975).

[44] M. L. Williams, R. F. Landel, and J. D. Ferry, J. Am. Chem. Soc. **77**, 3701 (1955).

[45] M. Holz, X. A. Mao, D. Seiferling, and A. Sacco, J. Chem. Phys. **104**, 669 (1996).

[46] D. Laage and J. T. Hynes, Science **311**, 832 (2006).

[47] D. Laage and J. T. Hynes, J. Phys. Chem. B **112**, 14230 (2008).

[48] F. Corsetti, P. Matthews, and E. Artacho, Sci. Rep. **6**, 18651 (2016).

[49] S. Strazdaite, J. Versluis, E. H. G. Backus, and H. J. Bakker, J. Chem. Phys. **140**, 054711 (2014).

[50] V. G. Artemov, I. A. Ryzhkin, and V. V. Sinitsyn, JETP Lett. **102**, 41 (2015).

[51] M. I. Ryzhkin, A. V. Klyuev, V. V. Sinitsyn, and I. A. Ryzhkin, JETP Lett. **104**, 248 (2016).

[52] I. A. Ryzhkin, M. I. Ryzhkin, M. M. Kashin, E. A. Galitskaya, and V. V. Sinitsyn, JETP Lett. **108**, 596 (2018).

[53] I. A. Ryzhkin, M. I. Ryzhkin, A. M. Kashin, E. A. Galitskaya, and V. V. Sinitsyn, Europhys. Lett. **126**, 36003 (2019).

[54] R. Zhang, Y. Chen, D. Troya, and L. A. Madsen, Macromolecules **53**, 3296 (2020).

[55] L. Onsager and L. K. Runnels, J. Chem. Phys. **50**, 1089 (1969).

[56] C. Jaccard, Phys. Kondens. Mater. **3**, 99 (1964).

[57] V. F. Petrenko and R. W. Whitworth, *Physics of Ice* (Oxford University Press, New York, 1999).

[58] R. Podeszwa and V. Buch, Phys. Rev. Lett. **83**, 4570 (1999).

[59] J. De Poorter, arXiv:1907.12479v3 [cond-mat.mtrl-sci] (2020).

[60] B. Geil, T. M. Kirschgen, and F. Fujara, Phys. Rev. B **72**, 014304 (2005).

[61] M. I. Ryzhkin, I. A. Ryzhkin, M. M. Kashin, and V. V. Sinitsyn, JETP Lett. **112**, 498 (2020).